RSC Advances

ROYAL SOCIETY OF CHEMISTRY

www.rsc.org/advances

SYNOPSIS

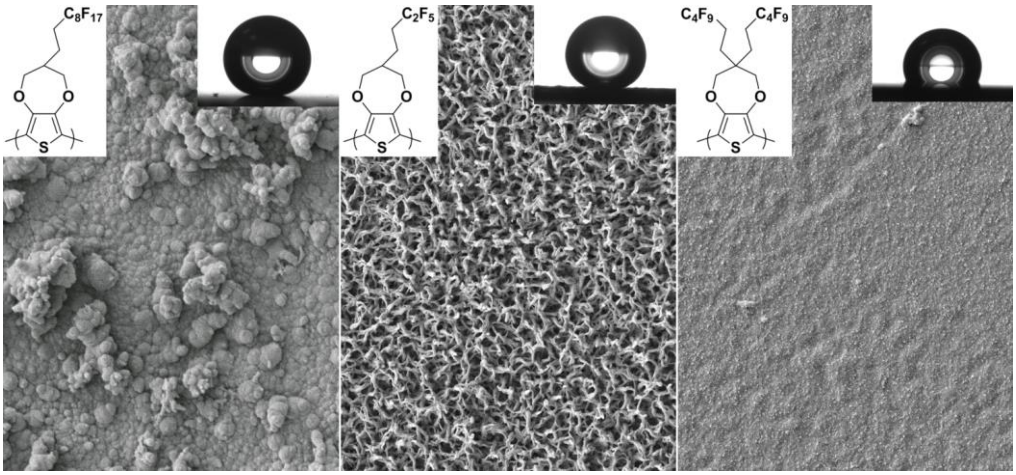

Journal Name

RSCPublishing

ARTICLE

Controlling electrodeposited conducting polymer nanostructures with the number and the length of fluorinated chains for adjusting superhydrophobic properties and adhesion

Cite this: DOI: 10.1039/x0xx00000x

Received 00th January 2012,
Accepted 00th January 2012

DOI: 10.1039/x0xx00000x

www.rsc.org/

Janwa El-Maiss, Thierry Darmanin, Frédéric Guittard*

Controlling the formation of surface nanostructures is highly important for various applications, and in particular for superhydrophobic properties. Here, taking 3,4-propylenedioxythiophene (ProDOT) as a model molecule, we study the influence of the decrease in the perfluorocarbon chain length or the use of two shorter perfluorocarbon chains on the formation of surface nanostructures and superhydrophobic by electropolymerization. Moreover, perfluorinated compounds, especially those with long perfluorocarbon chains, are extremely used in industry but the discovery of their persistence, bioaccumulation potential and toxicity alternatives have to be found. Hopefully, it seems that their effect is dependent on the perfluorinated chain length and that alternatives with shorter perfluorinated chains can be envisaged. Here, we show in the fabrication of superhydrophobic surfaces that the use of shorter perfluorocarbon chains can even, in certain conditions, lead to better properties. Superhydrophobic properties with extremely low hysteresis are obtained with long perfluorocarbon chains (C_8F_{17}) but very close properties are also obtained with short perfluorobutyl (C_4F_9) and even perfluoroethyl (C_2F_5) chains. Superoleophilic properties are obtained with C_2F_5 chains, whereas the highest oleophobic properties were elaborated with the C_4F_9 chains. This is due to a change in the surface morphology from cauliflower structures to nanofibers as the perfluorocarbon chain decreases. By contrast, the use of two shorter perfluorocarbon chains induces very high steric hindrance during the electropolymerization and as a consequence smoother surfaces with lower surface hydrophobicity. Hence, it is possible to form structured or smooth surfaces using one or two fluorinated chains, respectively.

Introduction

The bioinspired and biomimetic superhydrophobic materials are a very wide research subject from a theoretical[1] point of view and also for their potentials applications[2] for example in anti-corrosion,[3] self-cleaning textiles,[4] separation membranes,[5] microfluidic devices[6] or sensors/biosensors.[7] The preparation of superhydrophobic materials needs the presence of surface structures, often at the micro- and/or the nanoscale, while low surface energy materials are regularly used (fluorinated compounds and more precisely long perfluorocarbon chains).

Conducting polymers offers are unique materials for their opto-electronic properties[8] but also for the possible formation of nanostructures by self-assembly during their preparation.[9] For this purpose, due to the presence of hydrogen bonds, the polyaniline is very used to produce nanofibrous structures in solutions. However, for other conducting polymers such as 3,4-ethylenedioxythiophene (EDOT) derivatives it is often necessary to use nanostructured materials, surfactants or chemical seeds to induce the formation of nanostructured materials.[10]

Hopefully, the template-less the electrodeposition of conducting polymers is an excellent means to induce the growth of

nanostructures directly of substrates.[11] It consists, in "one-step", in a monomer oxidation, its polymerization and its deposition on a working electrode. This process is extremely fast and easy to implement while the surface morphology and roughness not only can be easily modified by the electrochemical parameters and also by tuning the monomer chemical structure.[12,13] For instance, because the conducting polymers can exist in different doping states, it is possible to modify the wettability properties by the introduction of dopant ions.[14–16] Furthermore, different substituents such as hydrocarbon or fluorocarbon chains can also be grafted to the monomer before polymerization.[17–19] Superhydrophobic properties were both reported using long hydrocarbon or fluorocarbon chains, but only the substitution by fluorocarbon allows to obtain also sometimes relatively high oleophobicity, which is an extremely important property for various applications such as the production of self-cleaning textiles and membranes.[20–22]

However, the use of perfluorinated substances has to be limited for industrial applications. The persistence, bioaccumulation potential and toxicity of perfluorinated substances such as long-chain perfluoroalkyl carboxylic acids (PFCAs) and perfluoroalkane sulfonic acids (PFSAs) are now well established and documented in the literature.[23–26] These compounds were found in the environment as well as in animals, plants and even in the human body. This was especially the case of perfluorinated substances with long perfluorocarbon chains (above 7 perfluoromethylene units).[27]

Hence, it becomes urgent to find alternatives to long perfluorocarbon chains. Indeed, the bioaccumulative potential being probably due to the interactions between membrane phospholipids and/or many proteins, these interactions are known to be dependent on the perfluorinated chain length.[24] Alternatives with short perfluorocarbon chains can, thus, be considered as non bioaccumulative compounds.

Here, the aim of this work is to show that, in the fabrication of nanostructured superhydrophobic conducting polymers with also high oleophobic properties, that it is not always necessary to use long perfluorocarbon chains. The work was realized using the 3,4-propylenedioxythiophene (ProDOT) core, which has exceptional polymerization capacity with the possibility to introduce various substituents.[28–30] The first strategy was to develop ProDOT derivatives bearing short fluorinated chain in the aim of studying the influence of the fluorinated chain length on the surface hydrophobicity and oleophobicity. One fluorinated chain containing a perfluorobutyl chain (C_4F_9), a perfluoroethyl chain (C_2F_5) and a trifluoromethyl group (CF_3) were each synthesized and the results were compared to those obtained with a long perfluorooctyl chain (C_8F_{17}). The second strategy was to introduce two short perfluorocarbon chains (C_4F_9, C_2F_5 and CF_3) which were then compared to their equivalent in mono-substituted chains. The two strategies are represented in **Scheme 1**. All these monomers were electropolymerized and the surface properties were characterized by scanning electron microscopy (SEM), optical profilometry and contact angle measurements.

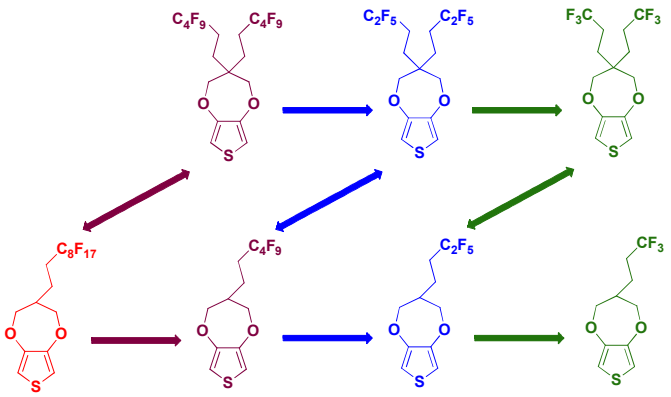

Scheme 1 Strategies used to reduce the bio-accumulative potential of monomers used for superhydrophobic and oleophobic materials.

Experimental

Monomer synthesis and characterization

The monomers were synthesized as described in **Scheme 2**. All chemicals were purchased from Sigma Aldrich and Fluorochem.

Synthesis of 1a-d. 1 eq. of sodium hydride (0.05 mol) were dissolved in 100mL anhydrous THF. Then, 2 eq. of diethyl malonate (0.1 mol) were added dropwise. After stirring for 30 min, 1 eq. of the corresponding iodo-fluorinated alkane was added and the mixture was heated under reflux for 24 hr. The solvent was evaporated under reduced pressure, then 40 mL of water were added, and the organic mixture was extracted by diethyl ether. The collected organic phases were washed using brine, dried over anhydrous $MgSO_4$. Purification was done by flash chromatography on silica gel (eluent: chloroform) to obtain the desired products.

1a: diethyl 2-(3,3,4,4,5,5,6,6,7,7,8,8,9,9,10,10,10-heptadecafluorodecyl)malonate. Yield: 81 %; Colourless liquid; δ_H(200 MHz, $CDCl_3$, ppm): 4.23 (q, $^3J_{H,H}$ = 7.1 Hz, 4H), 3.41 (t, $^3J_{H,H}$ = 7.0 Hz, 1H), 2.19 (m, 4H), 1.27 (t, $^3J_{H,H}$ = 7.1 Hz, 6H).

1b: diethyl 2-(3,3,4,4,5,5,6,6,6-nonafluorohexyl) malonate. Yield: 81%; Colourless liquid; δ_H(200 MHz, $CDCl_3$, ppm): 4.16 (q, $^3J_{H,H}$ = 7.1 Hz, 4H), 3.37 (t, $^3J_{H,H}$ = 7.0 Hz, 1H), 2.14 (m, 4H), 1.12(t, $^3J_{H,H}$ = 7.1 Hz, 6H).

1c: diethyl 2-(3,3,4,4,4-pentafluorobutyl)malonate. Yield: 70 %; Colourless liquid; δ_H(200 MHz, $CDCl_3$, ppm): 4.22 (q, $^3J_{H,H}$ = 7.1 Hz, 4H), 3.40(t, $^3J_{H,H}$ = 7.0 Hz, 1H), 2.18 (m, 4H), 1.28 (t, $^3J_{H,H}$ = 7.1 Hz, 6H).

1d: diethyl 2-(3,3,3-trifluoropropyl)malonate. Yield: 65 %; Colourless liquid; δ_H(200 MHz, $CDCl_3$, ppm): 4.22 (q, $^3J_{H,H}$ = 7.2 Hz, 4H), 3.39 (t, $^3J_{H,H}$ = 7.0 Hz, 1H), 2.21 (m, 4H), 1.27 (t, $^3J_{H,H}$ = 7.1 Hz, 6H).

Synthesis of 2a-c. 1eq. of t-BuONa, 1 eq. of 1b-d and 1 eq. of the corresponding iodo-fluorinated alkane were mixed in 100ml of THF. The reaction was heated under reflux for 48 hrs. The solvent was

evaporated under reduced pressure, then 40 mL of water were added, and the organic mixture was extracted by diethyl ether. The collected organic phases were washed using brine, dried over anhydrous Na_2SO_4. Purification was done by flash chromatography on silica gel (eluent: chloroform/cyclohexane 7/3) to obtain the products.

2a: diethyl 2,2-bis(3,3,4,4,5,5,6,6,6-nonafluorohexyl)malonate. Yield: 20 %; Colourless liquid; δ_H(200 MHz, $CDCl_3$, ppm): 4.26 (q, $^3J_{H,H}$ = 7.2 Hz, 4H), 2.14 (m, 8H), 1.27 (t, $^3J_{H,H}$ = 7.1 Hz, 6H).

2b: diethyl 2,2-bis(3,3,4,4,4-pentafluorobutyl)malonate. Yield: 20 %; Colourless liquid; δ_H(200 MHz, $CDCl_3$, ppm): 4.25(q, $^3J_{H,H}$ = 7.1 Hz, 4H), 2.07 (m, 8H), 1.27 (t, $^3J_{H,H}$ = 7.1 Hz, 6H).

2c: diethyl 2,2-bis(3,3,3-trifluoropropyl)malonate. Yield: 20 %; Colourless liquid; δ_H(200 MHz, $CDCl_3$, ppm): 4.24(q, $^3J_{H,H}$ = 7.1 Hz, 4H), 2.13(m, 8H), 1.28 (t, $^3J_{H,H}$ = 7.1 Hz, 6H).

Synthesis of 3a-d and 4a-c. The two ester functions were reduced by adding 1 eq. of the corresponding diester to a solution of 2.5 eq. of lithium aluminum hydride ($LiAlH_4$) (10 mmol) in 100 mL of diethyl ether ice cooled. The reaction mixture was stirred at 40 °C overnight. A mixture of NH_4Cl and diethyl ether was added, and then HCl (1N) was added to neutralize the remaining aluminum salts. Then, the aqueous mixture was extracted with diethyl ether. The collected organic phases were washed using brine, dried over anhydrous Na_2SO_4, affording to the product.

3a: 2-(3,3,4,4,5,5,6,6,7,7,8,8,9,9,10,10,10-heptadecafluorodecyl)propane-1,3-diol. Yield: 72%; Colourless liquid; δ_H(200 MHz, $CDCl_3$, ppm): 3.59 (dd, $^3J_{H,H}$ = 10.4, 4.5 Hz, 2H), 3.52 (dd, $^3J_{H,H}$ = 10.9, 4.9 Hz, 2H), 2.21 (m, 2H), 1.66 (m, 3H).

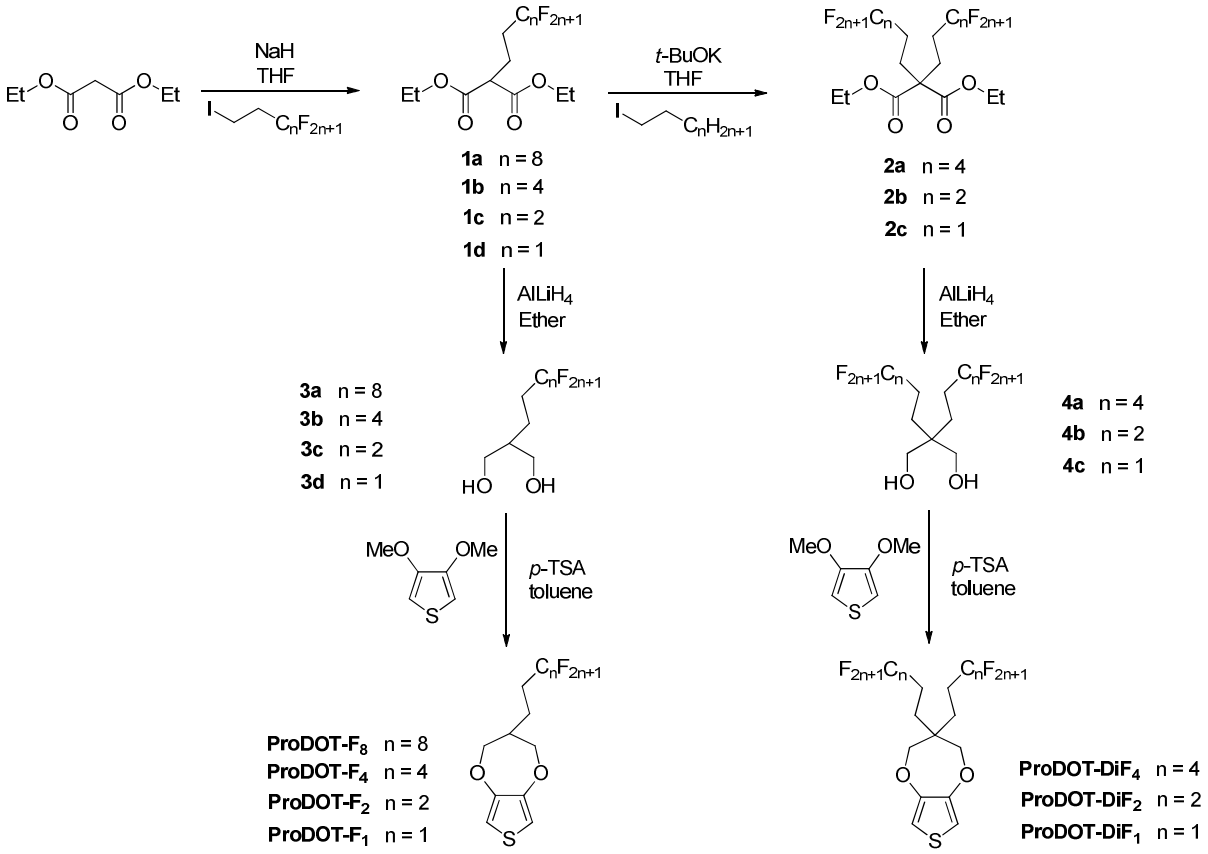

Scheme 1 Synthesis route to the monomers.

3b: 2-(3,3,4,4,5,5,6,6,6-nonafluorohexyl)propane-1,3-diol. Yield: 51%; Colourless liquid; δ_H(200 MHz, $CDCl_3$, ppm): 3.85 (dd, $^3J_{H,H}$ = 10.7, 3.8 Hz, 2H), 3.72 (dd, $^3J_{H,H}$ = 10.7, 6.0 Hz, 2H), 2.13 (m, 4H), 1.73 (m, 3H).

3c: 2-(3,3,4,4,4-pentafluorobutyl)propane-1,3-diol. Yield: 90%; Colourless liquid; δ_H(200 MHz, $CDCl_3$, ppm): 3.5 (dd, $^3J_{H,H}$ = 10.7, 3.8 Hz, 2H), 3.71 (dd, $^3J_{H,H}$ = 10.7, 6.0 Hz, 2H), 2.16 (m, 2H), 1.67 (m, 3H).

4a: 2,2-bis(3,3,4,4,5,5,6,6,6-nonafluorohexyl)propane-1,3-diol. Yield: 70%; Colourless liquid; δ_H(200 MHz, $CDCl_3$, ppm): 3.85 (dd, $^3J_{H,H}$ = 10.7, 3.8 Hz, 2H), 3.72 (dd, $^3J_{H,H}$ = 10.7, 6.0 Hz, 2H), 2.16 (m, 4H), 1.68(m, 4H).

4b: 2,2-bis-(3,3,4,4,4-pentafluorobutyl)propane-1,3-diol. Yield: 65%; Colourless liquid; δ_H(200 MHz, MeOD, ppm): 3.36 (s, 4H), 2.16 (m, 4H), 1.51 (m, 4H).

4c: 2,2-bis(3,3,3-trifluoropropyl)propane-1,3-diol. Yield: 60 %; Colourless liquid; δ_H(200 MHz, MeOD, ppm): 3.36 (s, 4H), 2.16 (m, 4H), 1.51 (m, 4H).

Synthesis of the monomers. The monomers were obtained by transetherification of 3,4-dimethoxythiophene by the corresponding diol (3 and 4). 3,4-dimethoxythiophene (1 eq., 2.6 mmol), the corresponding diol (1 eq., 2.6 mmol) and p-toluenesulfonic acid (0.3 mmol) were added to 30 mL of toluene. After stirring for 24 hr at 90°C, the products were purified by column chromatography gel (eluent: dichloromethane/cyclohexane 1:1).

ProDOT-F$_8$: 3-(3,3,4,4,5,5,6,6,7,7,8,8,9,9,10,10,10-heptadecafluorodecyl)-3,4-dihydro-2H-thieno[3,4-b][1,4]dioxepine. Yield: 35%; Crystalline solid; m.p. 85.3°C; δ_H(200 MHz, $CDCl_3$, ppm): 6.51 (s, 2H), 4.11 (dd, $^3J_{H,H}$ = 12.2, 3.4 Hz, 2H), 4.00 (dd, $^3J_{H,H}$ = 12.2, 5.3 Hz, 2H), 2.19 (m, 3H), 1.87 (m, 2H); δ_F(188 MHz, $CDCl_3$, ppm): –81.05, –115.23, –124.21, –126.08,; δ_C(50 MHz, $CDCl_3$, ppm): 150.0, 106.28, 73.74, 41.87, 28.6 (t, $^2J_{C,F}$ = 21.5 Hz), 18.70 (t, $^3J_{C,F}$ = 3.9 Hz); FTIR (main vibrations): ν = 3422, 2962, 1487, 1379, 1389, 1201, 1133, 1029, 996, 880; MS (70 eV): m/z (%): 602 (15) [M^+], 127 (35) [$C_4H_7OS^{+\bullet}$], 116 (100) [$C_4H_4O_2S^+$].

ProDOT-F$_4$: 3-(3,3,4,4,5,5,6,6,6-nonafluorohexyl)-3,4-dihydro-2H-thieno[3,4-b][1,4]dioxepine. Yield 20%; Crystalline solid; m.p. 48.78°C; δ_H(200 MHz, $CDCl_3$, ppm): 6.51 (s, 2H), 4.10 (dd, $^3J_{H,H}$ = 12.2, 3.4 Hz, 2H), 3.99 (dd, $^3J_{H,H}$ = 12.2, 5.2 Hz, 2H), 2.17 (m, 3H), 1.90 (m, 2H); δ_F(188 MHz, $CDCl_3$, ppm): –81.06, –114.91, –124.38, –126.08; δ_C(50 MHz, $CDCl_3$, ppm): 149.77, 106.06, 73.51, 41.63, 28.26 (t, $^2J_{C,F}$ = 22.6 Hz), 18.45 (t, $^3J_{C,F}$ = 3.6 Hz); FTIR (main vibrations): ν = 3108, 2974, 2908, 2866, 1491, 1452, 1379, 1239, 1218, 1195, 1134, 1010; MS (70 eV): m/z (%): 402 (100) [M^+], 127 (24) [$C_4H_7OS^{+\bullet}$], 116 (76) [$C_4H_4O_2S^+$].

ProDOT-F$_2$: 3-(3,3,4,4,4-pentafluorobutyl)-3,4-dihydro-2H-thieno[3,4-b][1,4]dioxepine. Yield: 35%; Colourless liquid, δ_H(200 MHz, $CDCl_3$, ppm): 6.51 (s, 2H), 4.10 (dd, $^3J_{H,H}$ = 12.2, 3.3 Hz, 2H), 4.00 (dd, $^3J_{H,H}$ = 12.3, 5.2 Hz, 2H), 2.13 (m, 3H), 1.85 (m, 2H); δ_F(188 MHz, $CDCl_3$, ppm): –85.27, –118.98; δ_C(50 MHz, $CDCl_3$, ppm): 149.20, 105.48, 72.92, 41.03, 27.54 (t, $^2J_{C,F}$ = 22.2 Hz), 18.00 (t, $^3J_{C,F}$ = 3.3 Hz); FTIR (main vibrations): ν = 3108, 2983, 1486, 1372, 1313, 1190, 1146, 1059, 893; MS (70 eV): m/z (%): 302 (100) [M^+], 127 (40) [$C_4H_7OS^{+\bullet}$], 116 (72) [$C_4H_4O_2S^+$].

ProDOT-F$_1$: 3-(3,3,4,4,4-pentafluorobutyl)-3,4-dihydro-2H-thieno[3,4-b][1,4]dioxepine. Yield: 30%; Colourless liquid, δ_H(200 MHz, $CDCl_3$, ppm): 6.51 (s, 2H), 4.09 (dd, $^3J_{H,H}$ = 12.1, 3.4 Hz, 2H), 3.98 (dd, $^3J_{H,H}$ = 12.1, 5.3 Hz, 2H), 2.22 (m, 3H), 1.82 (m, 2H); δ_F(188 MHz, $CDCl_3$, ppm): –66.81; δ_C(50 MHz, $CDCl_3$, ppm): 149.38, 105.61, 73.13, 40.83, 30.85 (t, $^2J_{C,F}$ = 29.0 Hz), 19.78 (q, $^3J_{C,F}$ = 3.0 Hz); FTIR (main vibrations): ν = 3449, 2970, 1455, 1382, 1358, 1224, 1133, 1036, 881; MS (70 eV): m/z (%): 252 (100) [M^+], 127 (27) [$C_4H_7OS^{+\bullet}$], 116 (69) [$C_4H_4O_2S^+$].

ProDOT-DiF$_4$: 3,3-bis(3,3,4,4,5,5,6,6,6-nonafluorohexyl)-3,4-dihydro-2H-thieno[3,4-b][1,4]dioxepine. Yield: 25%; Colourless liquid, δ_H(200 MHz, $CDCl_3$, ppm): 6.48 (s, 2H), 3.92 (s, 4H), 2.19 (m, 4H), 1.73 (m, 4H); δ_F(188 MHz, $CDCl_3$, ppm): –81.13, , –115.25, –124.24,–126.12; δ_C(50 MHz, $CDCl_3$, ppm): 148.34, 105.03, 75.25, 42.02, 24.60 (t, $^2J_{C,F}$ = 22.6 Hz), 22.38 (t, $^3J_{C,F}$ = 4.0 Hz), FTIR (main vibrations): ν = 3449, 2981, 1485, 1370, 1316, 1256, 1155, 1029, 893; MS (70 eV): m/z (%): 648 (63) [M^+], 127 (17) [$C_4H_7OS^{+\bullet}$], 116 (100) [$C_4H_4O_2S^+$].

ProDOT-DiF$_2$: 3,3-bis(3,3,4,4,4-pentafluorobutyl)-3,4-dihydro-2H-thieno[3,4-b][1,4]dioxepine. Yield: 28%; Colorless liquid, δ_H(200 MHz, $CDCl_3$, ppm): 6.47 (s, 2H), 3.92 (s, 4H), 2.10 (m, 4H), 1.71 (m, 4H); δ_F(188 MHz, $CDCl_3$, ppm): –85.27, –118.98; δ_C(50 MHz, $CDCl_3$, ppm): 148.30, 105.00, 75.59, 42.30, 24.46 (t, $^2J_{C,F}$ = 22.2 Hz), 23.06 (q, $^3J_{C,F}$ = 3.6 Hz); FTIR (main vibrations): ν = 3458, 2961, 1487, 1383, 1299, 1256, 1143, 1031, 897; MS (70 eV): m/z (%): 448 (76) [M^+], 127 (30) [$C_4H_7OS^{+\bullet}$], 116 (100) [$C_4H_4O_2S^+$].

ProDOT-DiF$_1$: 3,3-bis(3,3,3-trifluoropropyl)-3,4-dihydro-2H-thieno[3,4-b][1,4]dioxepine. Yield: 26%; Colorless liquid, δ_H(200 MHz, $CDCl_3$, ppm): 6.46 (s, 2H), 3.89 (s, 4H), 2.14 (m, 4H), 1.67 (m, 4H); δ_F(188 MHz, $CDCl_3$, ppm): –66.81; δ_C(50 MHz, $CDCl_3$, ppm): 148.32, 104.90, 75.28, 41.83, 26.50 (q, $^2J_{C,F}$ = 29.3 Hz), 24.35 (q, $^3J_{C,F}$ = 5.8 Hz),; FTIR (main vibrations): ν = 3415, 2961, 1487, 1382, 1232, 1258, 1120, 1026, 937; MS (70 eV): m/z (%): 348 (100) [M^+], 127 (24) [$C_4H_7OS^{+\bullet}$], 116 (76) [$C_4H_4O_2S^+$].

Electropolymerization conditions

An Autolab potentiostat (Metrohm) was used for the electropolymerization experiments. The experiments were performed inside a glass cell. 10 mL of anhydrous acetonitrile containing 0.1 M of electrochemical grade tetrabutylammonium perchlorate (Bu_4NClO_4) and 0.01 M of monomer were introduced and degassed under argon. The connection to the potentiostat was performed using three electrodes. A gold plate, on which the polymer is deposited, was used as working electrode, a carbon rod as counter-electrode and a saturated calomel electrode (SCE) as reference electrode. The cyclic voltammetry was chosen as deposition method because it leads to highly homogeneous and adherent films. The depositions were performed at a scan rate of 20 mV s-1 between -1.00 V vs SCE and 1.40-1.58 V following the monomer used for the experiments. To control the polymer growth, 1, 3 and 5 deposition scans were performed with each monomer.

Surface characterization

The scanning electron microscopy (SEM) using a 6700F microscope of JEOL was used to investigate the surface morphologies. The arithmetic (Ra) and quadratic (Rq) surface roughness were determined using a Wyko NT 1100 optical microscopy of Bruker. The roughness was determined on 182 x 239 μm^2 areas and using the working mode High Mag Phase Shift Interference (PSI), the objective 50X and the field of view (FOV) 0.5X.

For the surface wettability, three liquid probes of different surface tension were used to determine the surface hydrophobicity and oleophobicity: water (γ_{LV} = 72.8 mN/m), diiodomethane (γ_{LV} = 50.0 mN/m) and hexadecane (γ_{LV} = 27.6 mN/m). The contact angles were taken with a DSA30 goniometer of Krüss. The sessile drop method was used for the determination of the apparent contact angles (θ) while the tilted-drop method was used to determine the advancing and receding contact angles and as a consequence the hysteresis (H). The hysteresis was measured after surface inclination just before the droplet rolls off the surface. The maximum surface inclination is called sliding angle (α).

Results and Discussion

Electropolymerization conditions

The cyclic voltammetry is a fundamental tool for the study of conducting polymer growth and the substituent effects. Here, the studies were realized in anhydrous acetonitrile containing 0.1 M of Bu_4NClO_4. First of all, the cyclic voltammetry was used to determine the monomer oxidation potential ($E^{ox,m}$) by a single potential scan. $E^{ox,m}$ was found to be between 1.49 V and 1.56 V vs SCE for the mono-substituted monomers (PProDOT-F_n) and between 1.58 V and 1.65 V for the di-substituted monomers (PProDOT-DiF_n). Hence, the withdrawing effect induced by the grafting of the fluorinated chains on the 3-position increased significantly $E^{ox,m}$. Then, the polymers were electrodeposited by cyclic voltammetry between -1.00 V and a potential slightly lower than $E^{ox,m}$ and at a scan rate of 20 mV/s. Examples of cyclic voltammograms are shown in **Figure 1.**

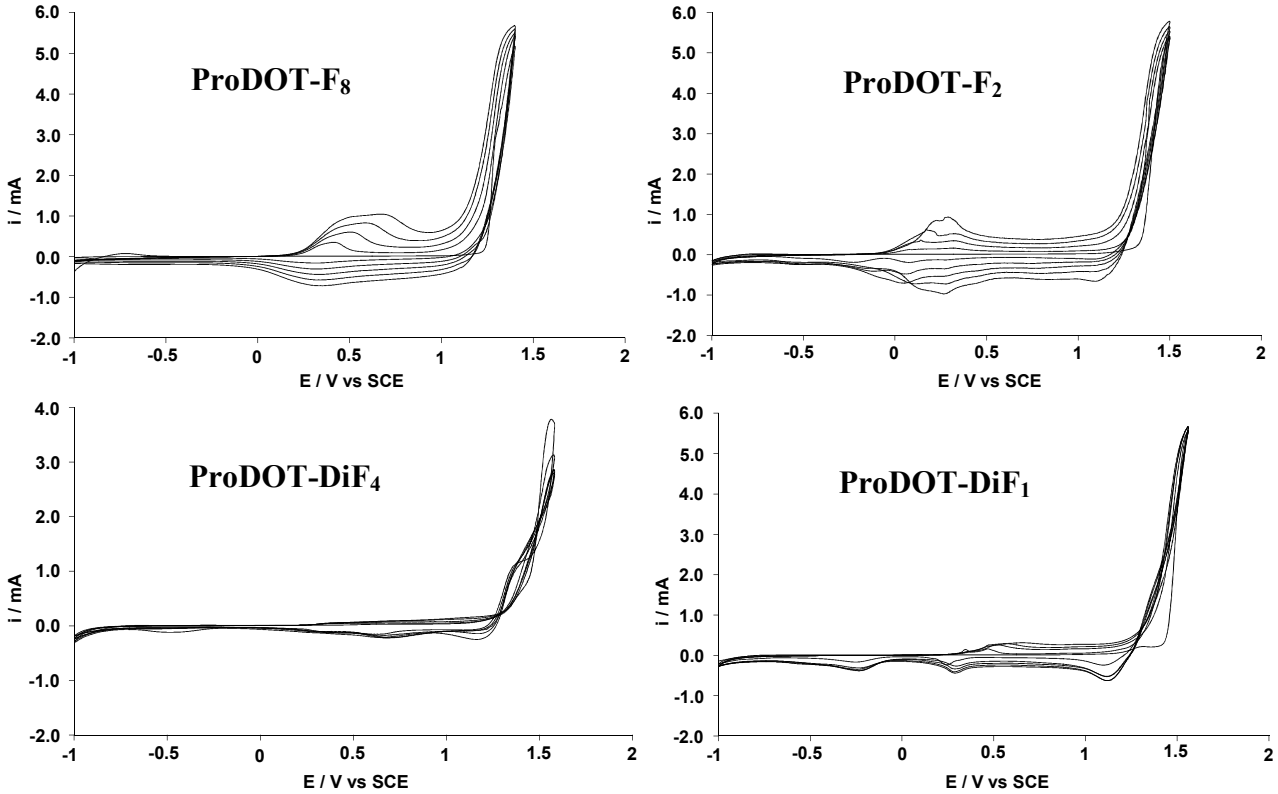

Fig. 1 Cyclic voltammetry of different monomer (0.01 M) recorded in anhydrous acetonitrile containing 0.1 M of Bu4NClO4; scan rate: 20 mV/s.

On the one hand, the mono-substituted monomers displayed a relatively homogeneous growth as indicated by a constant increase in the intensity of the polymer oxidation and reduction peaks. The effect of the mono-substitution is significant but not extremely important. The polymer oxidation potentials were found to be about 0.44 V for PProDOT-F_8, 0.20 V for PProDOT-F_4 and PProDOT-F_2, and 0.05 V for PProDOT-F_1. As expected, the fluorinated chains induced steric hindrance during the polymerization, which affects the polymer planarity and the polymer chain length. Indeed, the increase of the fluorinated chain length can have two effects. The first one is the increase in the steric hindrance due to the increase in the substituent size.

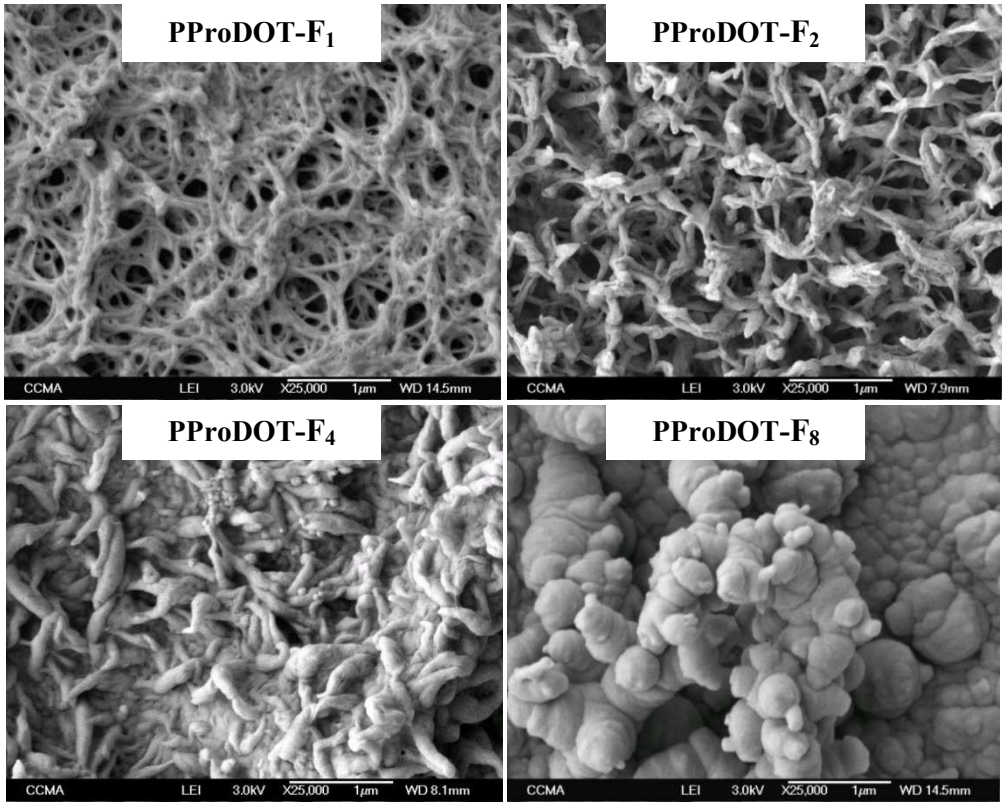

Fig. 2 SEM images of PProDOT-Fn polymers. Number of deposition scans: 3.

The second one is the decrease in the steric hindrance due to the decrease in the substituent mobility induces by intra/intermolecular interactions as described in the literature.[31,32] Indeed, the interactions between C_8F_{13} chains are very important but these interactions decrease as the fluorinated chain length.

On the other hand, the di-substitution induced very huge steric hindrance in comparison with the mono-substitution. The polymer oxidation potentials were about 0.40 V for PProDOT-DiF_4, and 0.47 V for PProDOT-DiF_2 and PProDOT-DiF_1. Moreover, the low intensity of the peaks observed by cyclic voltammetry of the di-substituted monomers indicated that the polymers are more soluble. Here, the di-substitution shortened the polymer chains while the presence of two fluorinated chains of high mobility also increased the polymer solubility.

Surface structures

The SEM images of the polymers for 3 deposition scans are given in **Figure 2, 3** and **4** and the mean roughness (Ra) and quadratic roughness (Rq) as a function of the number of deposition scans are available in **Table 1**. The Ra and Rq of each polymer increased as the number of deposition scans. The mono-substituted polymers PProDOT-F_n were extremely rough and it was also observed an increase in Ra and Rq as the alkyl chain length increased. Moreover, the SEM images (**Figure 3**) revealed a change in the surface morphology as a function of the alkyl chain length. The electrodeposition of PProDOT-F_1 formed horizontally aligned nanofibers in a nanoporous network while that of PProDOT-F_8 cauliflower structures without porosity. Interestingly, PProDOT-F_2 was composed of nanofibers rather vertically oriented with an extremely high amount of porosity between the fibers. Such structures are extremely interesting for superhydrophobic properties because the presence of porosity can lead to superhydrophobic properties with low adhesion.[33] By contrast, the di-substituted polymers PProDOT-DiFn were much smoother (Figure 3 and 4 and Table 1). Here, the di-substitution highly affected the presence of surfaces structures. For example, PProDOT-DiF_4 seems to be the smoother surfaces with only the presence of nanodots. These results can be explained with the literature data.[34,35] In recent advances, it was shown that during the electrodeposition of PEDOT in different solvents, the solubility of the oligomers formed in the first instance of the electropolymerization was a key parameter influencing the presence of surface structures. Structured surfaces were obtained in acetonitrile and smooth surfaces in dichloromethane due to a higher solubility of PEDOT in dichloromethane. In our work, the solvent used was always acetonitrile but we changed the monomers. The influence of the used substituents can have two effects: a direct influence on the polymer intrinsic hydrophobicity or an influence on the polymer chain length and as a consequence on the polymer solubility. Using the mono-substituted monomers ProDOT-Fn, even if the polymer chain length are affected by the fluorinated chain length, the changes in the surface morphology from nanofibers to cauliflower structures are mainly due to high increase in the polymer intrinsic hydrophobicity as the fluorinated chain length increases and as a consequence to a decrease in the solubility of the oligomers formed in the first instance of the electropolymerization.

Table 1 Mean roughness (Ra) and quadratic roughness (Rq) of polymer surfaces as a function of the number of deposition scans.

Polymers	1 scan		3 scans		5 scans	
	Ra	Rq	Ra	Rq	Ra	Rq
PProDOT-F_8	80	135	425	605	920	1165
PProDOT-F_4	14	18	417	550	675	895
PProDOT-F_2	33	43	325	455	460	710
PProDOT-F_1	13	17	182	235	320	415
PProDOT-DiF_4	18	24	61	81	210	285
PProDOT-DiF_2	49	62	52	68	110	175
PProDOT-DiF_1	38	49	54	66	175	230

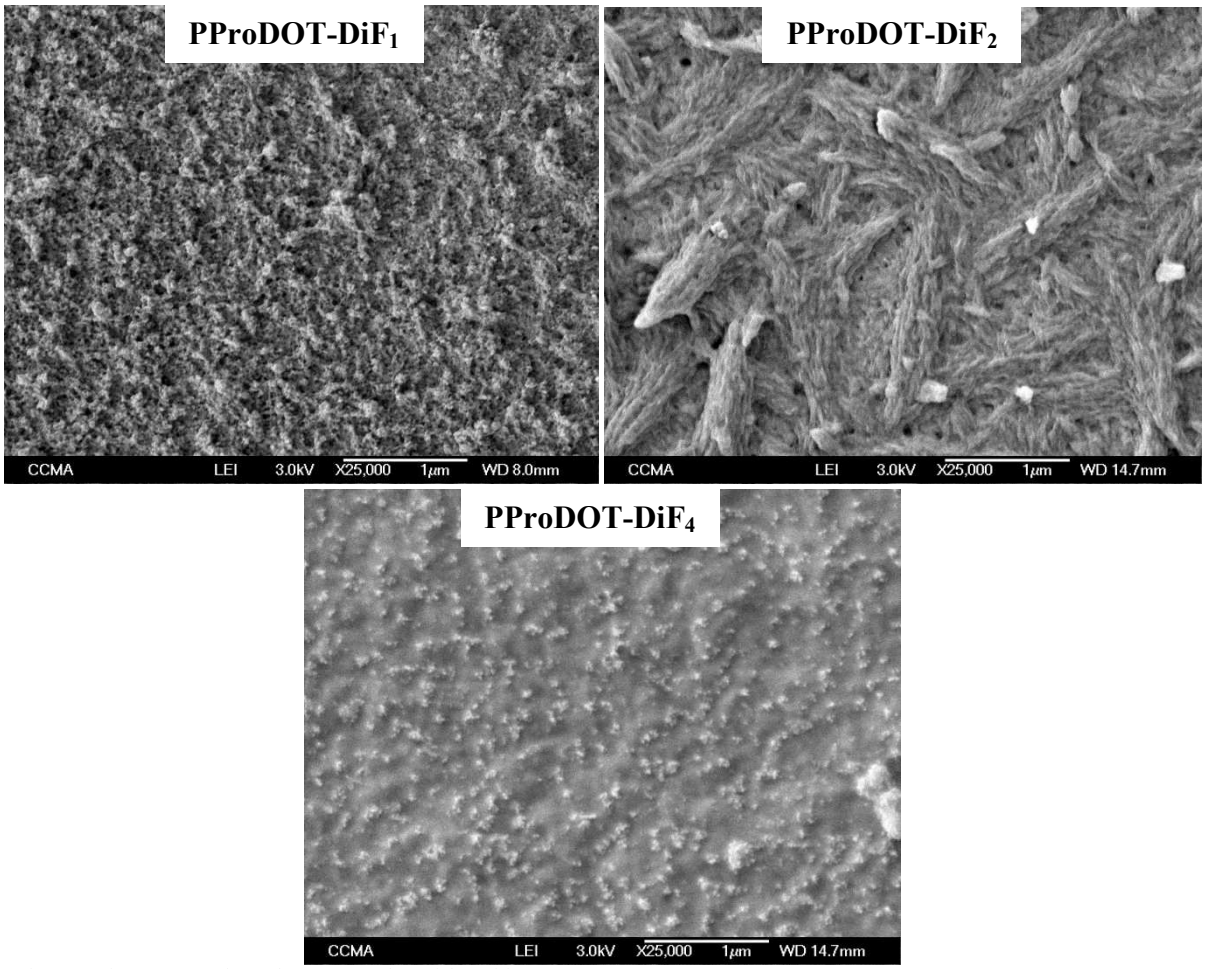

Fig. 3 SEM images of PProDOT-DiF_n polymers. Number of deposition scans: 3.

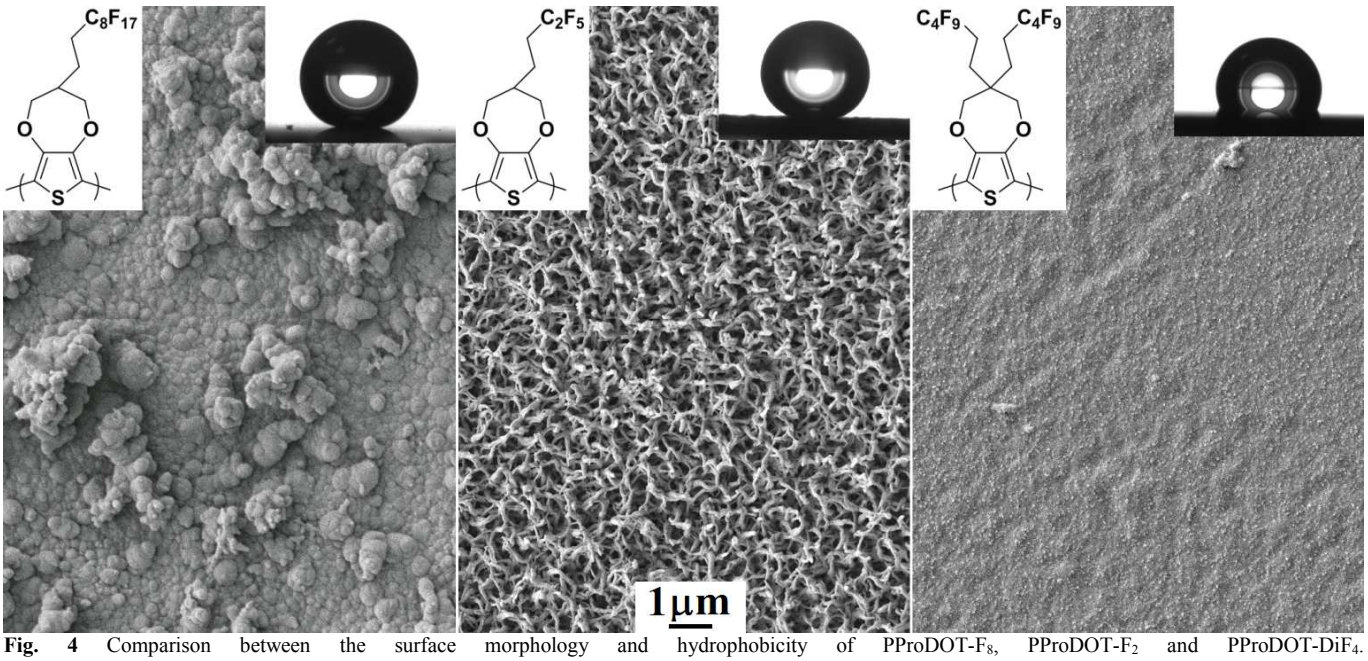

Fig. 4 Comparison between the surface morphology and hydrophobicity of PProDOT-F_8, PProDOT-F_2 and PProDOT-DiF_4.

Using the di-substituted monomers ProDOT-DiFn, the second effect became predominating. The di-substitution induced a very high decrease in the polymer chain length (cyclic voltammetry experiments) and as a consequence an increase in solubility of the oligomers formed in the first instance of the electropolymerization, which explains the obtaining of smoother surfaces.

Surface wettability

The apparent and dynamic contact angle measurements for the polymers electrodeposited by cyclic voltammetry are summarized in **Table 2** and **Figure 5.** The highest repellent surfaces were obtained for a number of scans of five and using the mono-substituted monomers ProDOT-F_n. Superhydrophobic properties with the lowest hysteresis (H) and sliding angles (α) were obtained for PProDOT-F_8 (H = 3.9 and α = 2.1) but low adhesion were also reported for PProDOT-F_4 (H = 9.9 and α = 7.9) and even PProDOT-F_2 (H = 8.5 and α = 6.5). Here, the decrease in the fluorinated chain from n = 8 to n = 2 had no significant effect on θ_{water} but slightly increased the water adhesion. Hence, it seems that the effect of the decrease in the fluorinated chain length is compensated by a change in the surface morphology more favourable to reach superhydrophobic properties (the nanofiber morphology induces a higher increase in θ_{water} than the cauliflower-like structures), as already reported in the literature.[36] The highest oleophobic properties were obtained for PProDOT-F_4, for which θ_{diiodo} = 136.7° and $\theta_{hexadecane}$ = 78.8° after 3 deposition scans. However, PProDOT-F_2 was superoleophilic.

The results can be explained using the Wenzel and Cassie-Baxter equations.[37,38] These equations being dependent on the Young angles (θ^Y),[39] it was necessary to prepare smooth surface for each polymers. Here, smooth surfaces for each polymer polymers were achieved by using another deposition method to better control the polymer growth. Smooth surfaces were obtained by electrodeposition at constant potential (1.40-1.58 V following the used monomer) and using an extremely low deposition charge (1 mC cm^{-1}) in order to have only the formation of a smooth and thin layer. The θ^Y for each polymer are given in **Table 3**. PProDOT-F_8 and PProDOT-F_4 were intrinsically hydrophobic ($\theta^Y_{water} > 90°$) while PProDOT-F_2 and PProDOT-F_1 were intrinsically hydrophilic ($\theta^Y_{water} < 90°$). However, these four polymers were also intrinsically oleophilic with (θ^Y_{diiodo} and $\theta^Y_{hexadecane} < 90°$).

These data are extremely interesting to understand the interface between the liquid and the substrate. When a liquid is in the "Wenzel state",[37] it penetrates in all the asperities of a rough surface. The Wenzel equation is $\cos\theta = r\cos\theta^Y$ where r corresponds to a roughness parameter. θ can be above θ^Y only if $\theta^Y > 90°$. Hence, the Wenzel equation can lead to superhydrophobic surfaces if $\theta^Y_{water} > 90°$ as well as superhydrophilic surfaces if $\theta^Y_{water} < 90°$. In the case of superhydrophobic properties, the hysteresis is important because the solid-liquid interface is increased by r.

By contrast, the Cassie-Baxter equation can predict $\theta > \theta^Y$ whatever θ^Y.[38] The Cassie-Baxter equation is $\cos\theta = r_f.f.\cos\theta^Y + f - 1$ where r*f* corresponds to the roughness ratio of the substrate wetted by the liquid, f corresponds to the solid fraction and (1 – f) corresponds to the air fraction, as described in the literature.[40,41] When a liquid follows the Cassie-Baxter equation, the liquid is in contact only with the top of the substrate asperities as well as on air trapped between the substrate and the liquid. Hence, the Cassie-Baxter would be favoured if the surface topography allows to trap a high amount of air. The Cassie-Baxter equation can lead to superhydrophobic properties with very low hysteresis is the surface is able to trap a high amount of air. That was the case of PProDOT-F_8 while the water penetrated a little more on

PProDOT-F_4 and PProDOT-F_2 leading to an increase in the water adhesion. However, when the surface tension of the liquid decreased (from 72.8 mN/m for water to 27.6 mN/m for hexadecane), the penetration became the lowest on PProDOT-F_4 and the highest on PProDOT-F_2.

Table 2 Apparent and dynamic contact angles of water, diiodomethane and hexadecane of the polymer surfaces.

Polymer	Number of Scans	θ_{water}	H_{water}	α_{water}	θ_{diiodo}	$\theta_{hexadecane}$
PProDOT-F_8	1	111.4	Sticking behaviour		111.5	73.8
	3	159.5	4.3	2.7	105.5	74.3
	5	158.6	3.9	2.1	107.1	71.6
PProDOT-F_4	1	116.3	Sticking behaviour		88.7	64.0
	3	159.0	9.9	7.9	136.7	78.8
	5	159.1	21.3	6.8	140.1	24.7
PProDOT-F_2	1	129.9	Sticking behaviour		107.8	50
	3	154.4	Sticking behaviour		120.9	0
	5	157.0	8.5	6.5	115.0	0
PProDOT-F_1	1	112.1	Sticking behaviour		109.4	71.1
	3	120.7	Sticking behaviour		111.1	70
	5	128.0	Sticking behaviour		110.0	69.5
PProDOT-DiF_4	1	111.7	Sticking behaviour		98.6	69.4
	3	110.9	Sticking behaviour		110.6	71.5
	5	115.3	Sticking behaviour		105.0	66
PProDOT-DiF_2	1	128.3	Sticking behaviour		106.0	69.5
	3	126.8	Sticking behaviour		100.6	73.7
	5	143.5	Sticking behaviour		91.5	69.6
PProDOT-DiF_1	1	107.5	Sticking behaviour		67.6	0
	3	114.2	Sticking behaviour		63.1	0
	5	140.7	Sticking behaviour		56.1	0

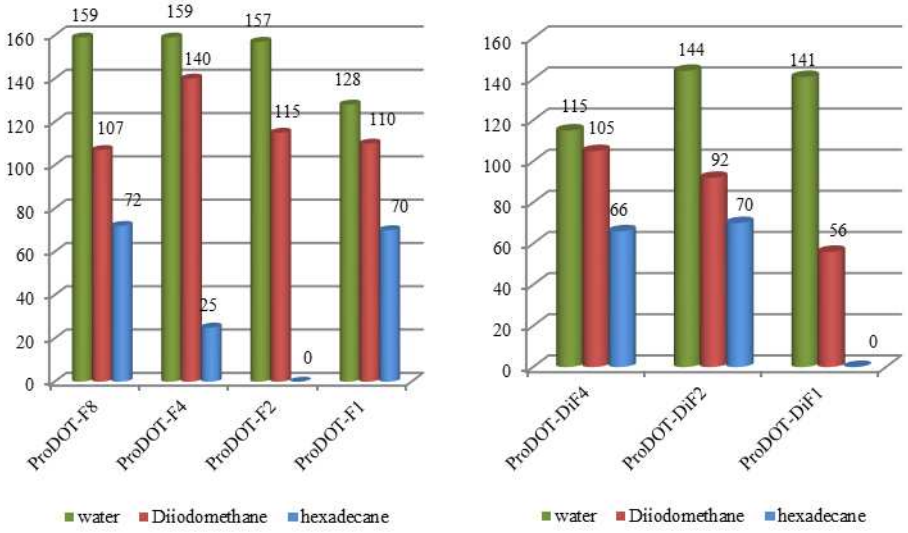

Fig. 5 Apparent contact angles of water, diiodomethane and hexadecane for the mono-substituted polymers PProDOT-Fn (on the left) and the di-substituted polymers PProDOT-DiFn (on the right); number of deposition scans: 5.

This can be explained in part by the change in the surface morphology from cauliflower structures for n = 8 to vertically aligned nanofibers for n = 2. The presence of vertically aligned nanofibers observed for PProDOT-F_2 highly increased the surface hydrophobicity but highly decreased the surface oleophobicity. By contrast, the presence of two fluorinated chains induced a significant decrease in θ_{water} while θ_{diiodo} and $\theta_{hexadecane}$ can increase or decrease, especially if the difference in the surface roughness and morphology is very important. Moreover, a water droplet deposited on PProDOT-DiF_1, PProDOT-DiF_2 and

PProDOT-DiF_4 remained stuck on them showing the extremely high water adhesion. The term parahydrophobic was proposed to explain this possibility.[42] Even if $\theta^Y_{water} < 90°$, it is possible to obtain $\theta_{water} > \theta^Y_{water}$ with an extremely high adhesion using the Cassie-Baxter equation if the penetration of the water inside the surface roughness is extremely important.

Table 3 Apparent and dynamic contact angles of water, diiodomethane and hexadecane of the "smooth" polymer surfaces.

Number of Scans	θ^Y_{water}	θ^Y_{diiodo}	$\theta^Y_{hexadecane}$
PProDOT-F_8	93.3	54.6	31.8
PProDOT-F_4	97.9	67.5	38.2
PProDOT-F_2	84.3	48.2	22.1
PProDOT-F_1	87.8	48.1	27.8
PProDOT-DiF_4	105.1	65.4	38.0
PProDOT-DiF_2	81.9	41.4	11.5
PProDOT-DiF_1	73.2	28.4	0.0

Conclusion

Here, taking 3,4-propylenedioxythiophene (ProDOT) as a model molecule, we showed the possibility to control the formation of surface nanostructures and hydrophobic properties by modifying the length or the number of perfluorocarbon chains. Superhydrophobic properties with extremely low hysteresis could be obtained with long perfluorocarbon chains (C_8F_{17}) but very close properties with short perfluorobutyl (C_4F_9) and even perfluoroethyl (C_2F_5) chains. If superoleophilic properties were obtained with C_2F_5 chains, the highest oleophobic properties were obtained with C_4F_9 chains. This was due to a change in the surface morphology from cauliflower structures to nanofibers as the perfluorocarbon chain decreases. However, the use of two shorter perfluorocarbon chains led to very high steric hindrance during the electropolymerization and as a consequence smoother surfaces with lower surface hydrophobicity. Hence, it is now possible to prepare structured or smooth surfaces using one or two fluorinated chains, respectively.

Acknowledgements

This project was supported by JSPS [KAKENHI, Grant-in-Aid for Young Scientists (A), No. 23685034], RCUK [through EPSRC EP/K020676/1] and ANR-13-G8ME-0003 under the G8 Research Councils Initiative on Multilateral Research Funding - G8-2012. The group also thanks Jean-Pierre Laugier (CCMA, Univ. Nice Sophia Antipolis) for the SEM analyses.

Notes

Corresponding author:
Frederic.Guittard@unice.fr
Tel: (+33)4 92 07 61 59
Univ. Nice Sophia Antipolis, CNRS, LPMC, UMR 7336, 06100 Nice, France

References

1 H. Bellanger, T. Darmanin, E. Taffin De Givenchy and F. Guittard, *Chem. Rev.*, 2014, **114**, 2694.
2 T. Darmanin and F. Guittard, *J. Mater. Chem. A*, 2014, **2**, 16319.
3 C. J. Weng, C. H. Chang, C. W. Peng, S. W. Chen, J. M. Yeh, C. L. Hsu and Y. Wei, *Chem. Mater.*, 2011, **23**, 2075.
4 D. Tian, X. Zhang, X. Wang, J. Zhai and L. Jiang, *Phys. Chem. Chem. Phys.*, 2011, **13**, 14606.
5 a) Z. Xue, Y. Cao, N. Liu, L. Feng and L. Jiang, *J. Mater. Chem. A*, 2014, **2**, 2445; b) B. Wang, W. Liang, Z. Guo and W. Liu, *Chem. Soc. Rev.*, 2015, **44**, 336.
6 G. D. Bixler and B. Bhushan, *Nanoscale*, 2014, **6**, 76.
7 a) H. Li, J. Wang, L. Yang and Y. Song, *Adv. Funct. Mater.*, 2008, **18**, 3258; b) A. Ressine, G. Marko-Varga and T. Laurell, *Biotechnol. Annu. Rev.*, 2007, 13, 149.
8 P. M. Beaujuge and J. R. Reynolds, *Chem. Rev.*, 2010, **110**, 268.
9 a) J. Huang, S. Virji, B. H. Weiller and R. B. Kaner, *J. Am. Chem. Soc.*, 2003, **125**, 314; b) Y. Zhu, D. Hu, M.X. Wan, L. Jiang and Y. Wei, *Adv. Mater.*, 2007, **19**, 2092; c) Y. Zhu, J. Li, M. Wan and L. Jiang, *Macromol. Rapid Commun.*, 2008, **29**, 239.
10 a) A. K. C. Gallegos and M. E. Rincón, *J. Power Sources*, 2006, **162**, 743; b) M. G. Han and S. H. Foulger, *Small*, 2006, **2**, 1164; b) X. Zhang, A. G. MacDiarmid and S. K. Manohar, *Chem. Commun.*, 2005, 5328.
11 a) T. Darmanin and F. Guittard, *Prog. Polym. Sci.*, 2014, **39**, 656; b) H. Yan, K. Kurogi, H. Mayama and K Tsujii, *Angew. Chem., Int. Ed.*, 2005, **44**, 3453; c) L. Xu, W. Chen, A. Mulchandani and Y. Yan, *Angew. Chem., Int. Ed.*, 2005, 44, 6009.
12 C. Li, H. Bai and G. Shi, *Chem. Soc. Rev.*, 2009, **38**, 2397;
13 Y.-Z. Long, M.-M. Li, C. Gu, M. Wan, J.-L. Duvail, Z. Liu and Z. Fan, *Prog. Polym. Sci.*, 2011, 36, 1415.
14 P. Lin, F. Yan and H. L. W. Chan, *Langmuir*, 2009, **25**, 7465.
15 J. Zang, C. M. Li, S. J. Bao, X. Cui, Q. Bao and C. Q. Sun, *Macromolecules*, 2008, **41**, 7053.
16 L. Xu, W. Chen, A. Mulchandani and Y. Yan, *Angew. Chemie - Int. Ed.*, 2005, **44**, 6009.
17 T. Darmanin and F. Guittard, *J. Am. Chem. Soc.*, 2009, **131**, 7928.
18 T. Darmanin and F. Guittard, *J. Am. Chem. Soc.*, 2011, **133**, 15627.
19 S. C. Luo, J. Sekine, B. Zhu, H. Zhao, A. Nakao and H. H. Yu, *ACS Nano*, 2012, **6**, 3018.
20 S. Pan, A. K. Kota, J. M. Mabry and A. Tuteja, *J. Am. Chem. Soc.*, 2013, **135**, 578.
21 R. Dufour, M. Harnois, Y. Coffinier, V. Thomy, R. Boukherroub and V. Senez, *Langmuir*, 2010, **26**, 17242.
22 T. Darmanin, J. Tarrade, E. Celia and F. Guittard, *J. Phys. Chem. C*, 2014, **118**, 2052.
23 M. I. Gomis, Z. Wang, M. Scheringer and I. T. Cousins, *Sci. Total Environ.*, 2015, **505**, 981.
24 C. A. Ng and K. Hungerbuehler, *Environ. Sci. Technol.*, 2014, 48, 4637.
25 A. A. Rand, J. P. Rooney, C. M. Butt, J. N. Meyer and S. A. Mabury, *Chem. Res. Toxicol.*, 2014, **27**, 42.

26 A. Glynn, U. Berger, A. Bignert, S. Ullah, M. Aune, S. Lignell and P. O. Darnerud, *Environ. Sci. Technol.*, 2012, **46**, 9071.
27 J. M. Conder, R. a Hoke, W. De Wolf, M. H. Russell and R. C. Buck, *Environ. Sci. Technol.*, 2008, **42**, 995.
28 C. L. Gaupp, D. M. Welsh and J. R. Reynolds, *Macromol. Rapid Commun.*, 2002, **23**, 885.
29 T. Darmanin, C. Mortier, J. Eastoe, M. Sagisaka and F. Guittard, *RSC Adv.*, 2014, **4**, 35708.
30 T. Dey, M. a. Invernale, Y. Ding, Z. Buyukmumcu and G. a. Sotzing, *Macromolecules*, 2011, **44**, 2415.
31 K. Honda, M. Morita, H. Otsuka and A. Takahara, *Macromolecules*, 2005, **38**, 5699.
32 K. Honda, M. Morita, O. Sakata, S. Sasaki and A. Takahara, *Macromolecules*, 2010, **43**, 454.
33 D. Chandra and S. Yang, *Acc. Chem. Res.*, 2010, **43**, 1080.
34 E. Poverenov, M. Li, A. Bitler and M. Bendikov, *Chem. Mater.*, 2010, **22**, 4019.
35 C. Mortier, T. Darmanin and F. Guittard, *Adv. Eng. Mater.*, 2014, **16**, 1400.
36 M. Wolfs, T. Darmanin and F. Guittard, *RSC Adv.*, 2013, **3**, 647.
37 R. N. Wenzel, *J. Ind. Eng. Chem.*, 1936, **28**, 988.
38 A. B. D. Cassie and S. Baxter, *Trans. Faraday Soc.*, 1944, 40, 546.
39 T. Young, *Phil. Trans. R. Soc. Lond.*, 1805, 95, 65.
40 A. Marmur, *Soft Matter*, 2013, **9**, 7900.
41 A. Marmur, *Langmuir*, 2003, **19**, 8343.
42 A. Marmur, *Soft Matter*, 2012, **8**, 6867.